



## A multidisciplinary effort to assign realistic source parameters to models of volcanic ash-cloud transport and dispersion during eruptions

L.G. Mastin<sup>a,\*</sup>, M. Guffanti<sup>b</sup>, R. Servranckx<sup>c</sup>, P. Webley<sup>d</sup>, S. Barsotti<sup>e</sup>, K. Dean<sup>d</sup>, A. Durant<sup>f</sup>, J.W. Ewert<sup>a</sup>, A. Neri<sup>e</sup>, W.I. Rose<sup>g</sup>, D. Schneider<sup>h</sup>, L. Siebert<sup>i</sup>, B. Stunder<sup>j</sup>, G. Swanson<sup>k</sup>, A. Tupper<sup>l</sup>, A. Volentik<sup>m</sup>, C.F. Waythomas<sup>h</sup>

<sup>a</sup> U.S. Geological Survey, Cascades Volcano Observatory, 1300 SE Cardinal Court, Bldg. 10, Suite 100, Vancouver, WA 98683, USA

<sup>b</sup> U.S. Geological Survey Reston, Virginia, USA

<sup>c</sup> Canadian Meteorological Centre, Québec, Canada

<sup>d</sup> Geophysical Institute, University of Alaska Fairbanks, USA

<sup>e</sup> Istituto Nazionale di Geofisica e Vulcanologia, Sezione di Pisa, Pisa, Italy

<sup>f</sup> Department of Earth Sciences, University of Bristol, England

<sup>g</sup> Department of Geological and Engineering Sciences, Michigan Technological University, USA

<sup>h</sup> USGS Alaska Volcano Observatory, Anchorage, AK

<sup>i</sup> Smithsonian Institution, Washington, D.C., USA

<sup>j</sup> Air Resources Laboratory, National Oceanic and Atmospheric Administration, Silver Spring, MD

<sup>k</sup> National Oceanic and Atmospheric Administration, Camp Springs, MD, USA

<sup>l</sup> Bureau of Meteorology, Darwin, Casuarina, NT, Australia

<sup>m</sup> Department of Geology, University of South Florida, Tampa, FL, USA

### ARTICLE INFO

Available online 23 January 2009

#### Keywords:

volcanic eruption  
aircraft  
volcanic plumes  
ash clouds

### ABSTRACT

During volcanic eruptions, volcanic ash transport and dispersion models (VATDs) are used to forecast the location and movement of ash clouds over hours to days in order to define hazards to aircraft and to communities downwind. Those models use input parameters, called “eruption source parameters”, such as plume height  $H$ , mass eruption rate  $M$ , duration  $D$ , and the mass fraction  $m_{63}$  of erupted debris finer than about  $4\phi$  or  $63\ \mu\text{m}$ , which can remain in the cloud for many hours or days. Observational constraints on the value of such parameters are frequently unavailable in the first minutes or hours after an eruption is detected. Moreover, observed plume height may change during an eruption, requiring rapid assignment of new parameters. This paper reports on a group effort to improve the accuracy of source parameters used by VATDs in the early hours of an eruption. We do so by first compiling a list of eruptions for which these parameters are well constrained, and then using these data to review and update previously studied parameter relationships. We find that the existing scatter in plots of  $H$  versus  $M$  yields an uncertainty within the 50% confidence interval of plus or minus a factor of four in eruption rate for a given plume height. This scatter is not clearly attributable to biases in measurement techniques or to well-recognized processes such as elutriation from pyroclastic flows. Sparse data on total grain-size distribution suggest that the mass fraction of fine debris  $m_{63}$  could vary by nearly two orders of magnitude between small basaltic eruptions ( $\sim 0.01$ ) and large silicic ones ( $> 0.5$ ). We classify eleven eruption types; four types each for different sizes of silicic and mafic eruptions; submarine eruptions; “brief” or Vulcanian eruptions; and eruptions that generate co-ignimbrite or co-pyroclastic flow plumes. For each eruption type we assign source parameters. We then assign a characteristic eruption type to each of the world’s  $\sim 1500$  Holocene volcanoes. These eruption types and associated parameters can be used for ash-cloud modeling in the event of an eruption, when no observational constraints on these parameters are available.

Published by Elsevier B.V.

### 1. Introduction

The May 18, 1980, eruption of Mount St. Helens was perhaps the most thoroughly documented of the past century in terms of media coverage and yield of scientific data. Among all of the human drama,

spectacular images, and dramatic events of that day were two incidents that, surprisingly, received scant attention. A McDonnell–Douglas DC-9-30 flying through the ash cloud suffered damage to engine parts, surface abrasion to the windshield, and a clogged hydraulic system (Miller and Casadevall, 2000; International Civil Aviation Organization, 2001); and a Boeing 747 sustained damage from ash while parked on the ground. A week later on May 25, a C-130 Hercules flew through the cloud of a smaller eruption while en route

\* Corresponding author.

E-mail address: [lgmastin@usgs.gov](mailto:lgmastin@usgs.gov) (L.G. Mastin).

from Tacoma, Washington to Portland, Oregon. The plane suffered temporary engine failure, permanent engine damage, and contamination to air handling systems, hydraulic lines, and pitot tubes (Miller and Casadevall, 2000; International Civil Aviation Organization, 2001). A day later, two Boeing 727 Trijet transports also encountered the ash cloud and suffered engine damage. The May 25 incident was the first documented encounter resulting in jet power loss. The May 18 DC-9 incident was the first known to involve engine damage (International Civil Aviation Organization, 2001).

Despite these incidents, the international aviation community paid little attention to the hazards of ash clouds until October 1982, when four Boeing 747s flew through clouds emanating from Galunggung volcano, Indonesia (Miller and Casadevall, 2000). The Galunggung encounters prompted the International Civil Aviation Organization's (ICAO's) Air Navigation Commission to develop interim guidelines for disseminating information on volcanic activity to pilots. In 1987, ICAO created the International Airways Volcano Watch (IAVW) to develop

mitigation procedures and, during the 1990s, established nine Volcanic Ash Advisory Centers (VAACs) around the world whose purpose is to issue specialized advisories to the aviation community. VAACs are composed of government institutions with the capability and authority to evaluate ash-cloud models, analyze satellite data, and issue meteorological weather advisories (SIGMETs) that may include ash-cloud advisories.

The VAACs use volcanic ash transport and dispersion (VATD) models, such as PUFF (Searcy et al., 1998), HYSPLIT (Draxler and Hess, 1998), CANERM (D'Amours et al., 1998), NAME (Jones et al., 2007), and MEDIA (Piedelievre et al., 1990), to forecast the paths of ash clouds so that they can be avoided by aircraft. The models are also useful in forecasting areas on the ground most likely to be impacted by tephra fall. These models require input parameters such as plume height, mass eruption rate, tephra-size distribution, and the duration of the eruption. Since the late 1990s, IAVW has recognized that more accurate source parameters are needed to improve model accuracy, especially in

**Table 1**

Eruption source parameters for well-studied eruptions. Variables include plume height  $H$ , erupted volume  $V$ , mass eruption rate  $M$ , and duration  $D$ . The mass eruption rate is calculated by multiplying the erupted volume by density to arrive at an erupted mass, and then dividing the erupted mass by the duration. Plume heights are annotated with a letter, which indicates the method by which plume height was estimated: "v"=visual observation from the ground or an airplane; "r"=radar; "s"=satellite images; "i" = isopleth data. For silicic eruptions, column 3 indicates the magma type; r=rhyolite, d=dacite, a=andesite. Letters in parentheses indicate subordinate magma types. Observations that form the basis for these values are described in Mastin et al. (in preparation).

Volcano	Date of onset	Magma type	VEI	$H$ , (km)	$V$ , (km <sup>3</sup> ) DRE	$M$ , (kg/s)	$D$ , (h)	Reference
<i>Silicic and andesitic eruptions</i>								
St. Helens	3/8/2005	d	2	9v	1e-04	4e05	0.5	1,2
St. Helens	7/22/1980	d	2	10.3r	0.001	1.4e06	0.45	3
St. Helens	5/25/1980	d	3	10.2r	0.016	2e07	<0.5	3
St. Helens	6/12/1980	d	3	9.6r	0.017	2e07	0.5	3
Pinatubo, Philippines	6/12/1991	d	3	17.5r	0.0056	6e06	0.63	4,5,40
Ruapehu, NZ	6/17/1996	a	3	5.7s	0.002	2e05	6.5	12,13
Redoubt, USA	12/15/1989	a	3	9v	0.008	4–7e06	1.03	14, 15
Nevado del Ruiz, Colombia	11/13/1985	a,d	3	26i	0.014	3e07	0.3	16
Spurr, USA	6/27/1992	a	3	11.3r	0.012	2e06	4.4	17,18,19
Spurr, USA	8/18/1992	a	3	10.5r	0.014	3e06	3.5	17,18,19
Spurr, USA	9/17/1992	a	3	10.7r	0.015	3e06	3.6	17,18,19
Hekla, 1970	5/5/1970	a	3	12–16v	0.017	6e06	2	20
Hekla, 1980	8/17/1980	a	3	15v	0.019	2e06	5	21
Reventador, Ecuador	11/3/2002	a	4	17v	0.12	1e07	22	22
Hekla, 1947	3/29/1947		4					
brownish-gray ash		a		28v	0.034	4.6e07	0.5	
brownish-black ash		a		8–25v	0.013	1.6e07	0.5	23
Soufrière, St. Vincent	5/7/1902	a,d	4	14v	0.14	3–4e07	2.5–3.5	24,25
El Chichón A, Mexico	3/29/1982	a	5	20i	0.30	3.5e07	5	26
El Chichón B, Mexico	4/4/1982 0135 GMT	a	5	24i	0.39	6.0e07	4	26
El Chichón C, Mexico	4/4/1982 1122 GMT	a	5	22i	0.40	4.0e07	7	26
Hudson, Chile	8/12/1991	a	5	12–18v	3.0	7e07	31	27,28
St. Helens	5/18/1980	d	5	13.5r	0.2	2e07	9	3,6
Quizapu, Chile	4/10/1932	d	6	27–30i	4.0	1.5e08	18	7
Novarupta	6/6/1912		6					
Episode I		r,d,(a)		23.5i	2.94	1.2e08	16	
Episode II		d		22.5i	1.96	5.2e07	26	
Episode III		d,(a)		19i	1.63	1.1e08	10	8
Pinatubo, Philippines	6/15/1991	d	6	35–40s	0.8–1.6	2–4e08	3	9,10,11,40
Santa Maria, Guatemala	10/24/1902	a,(d)	6	34i	3.3	5–7e07	24–36	29,30,31
<i>Basaltic eruptions</i>								
Etna, 2001	7/19/2001		2	0.5–2.5v	9e–04	6e03	115	32
Cerro Negro, 1995	11/19/1995		2	2–2.5v	1.3e–03	9.4e03	~100	33
Cerro Negro, 1992	4/9/1992		3	2.8–6.8v	0.0094	3e05	~21	33
Izu–Oshima	11/21/1986	a,(a)	3	10s,r,v	0.0045	8e05	3	41
Fuego, 1971	9/14/1971		3	10v	0.03	1.7e06	12	34,35
Miyakejima, Japan	8/18/2000		3	15.5r	0.0042	1.2e06	3.4	36,37,38
Fuego, 1974	10/14/1974		4	10v	0.02	3e06	5	39

Information sources:

<sup>1</sup>Mastin (2007); <sup>2</sup>Scott et al. (in press); <sup>3</sup>Sarna-Wojcicki et al. (1981); <sup>4</sup>Paladio-Melosantos et al., 1996; <sup>5</sup>Hoblitt et al. (1996); <sup>6</sup>Durant et al. (2009); <sup>7</sup>Hildreth and Drake (1992); <sup>8</sup>Fierstein and Hildreth (1992); <sup>9</sup>Koyaguchi (1996); <sup>10</sup>Koyaguchi and Ohno (2001a); <sup>11</sup>Holasek et al. (1996); <sup>12</sup>Prata and Grant (2001); <sup>13</sup>Bonadonna and Houghton (2005); <sup>14</sup>Miller and Chouet (1994); <sup>15</sup>Scott and McGimsey (1994); <sup>16</sup>Naranjo et al. (1986); <sup>17</sup>Neal et al. (1995); <sup>18</sup>Eichelberger et al. (1995); <sup>19</sup>(McGimsey et al., 2001) <sup>20</sup>Thorarinsson and Sigvaldason (1971); <sup>21</sup>Gronvold et al. (1983); <sup>22</sup>Smithsonian Institution (2002); <sup>23</sup>Thorarinsson (1949); <sup>24</sup>Anderson and Flett (1903); <sup>25</sup>Carey and Sigurdsson (1978); <sup>26</sup>Carey and Sigurdsson (1986); <sup>27</sup>Scasso et al. (1994); <sup>28</sup>Naranjo et al. (1993); <sup>29</sup>Rose (1972); <sup>30</sup>Carey and Sparks (1986); <sup>31</sup>Anderson (1908); <sup>32</sup>Scollo et al. (2007); <sup>33</sup>Hill et al. (1998); <sup>34</sup>Bonis and Salazar (1973); <sup>35</sup>Rose et al. (1973); <sup>36</sup>Tupper et al. (2004); <sup>37</sup>Nakada et al. (2005); <sup>38</sup>Geshi et al. (2002); <sup>39</sup>Rose et al. (2008); <sup>40</sup>Pallister et al. (1992); <sup>41</sup>Mannen (2006).

the first hours of an eruption when few observations may be available. In the spring of 2007, a multidisciplinary group consisting of the authors of this report convened to develop a method of assigning eruption parameters in real time to improve the accuracy of VATD models. We analyzed variations in plume height, eruption rate, duration, grain-size distribution, and erupted volume among eruptions described in the literature, and used those relationships to identify categories of eruption and their associated source parameters.

## 2. Source parameters based on well-documented eruptions

Volcanic events that threaten air traffic vary widely in size and style. Nevertheless, some characteristic eruption parameters display broad systematic relationships: for example plume height increases with eruption rate; and grain-size generally decreases with increasing silica content. But not all relationships are systematic. The duration of eruptions may decrease or vary non-systematically with eruption size or magma type, for example. Average grain size, while generally decreasing with increasing silica content, may also decrease with increasing incidence of pyroclastic flows (Darteville et al., 2002).

### 2.1. Observations and uncertainties

To examine these relationships more closely, we compiled published data on plume height, erupted volume or mass, and duration for a few dozen well-documented eruptions (Table 1). The list is not exhaustive but provides a large enough sampling to examine relationships and their uncertainties. The observations from which these numbers were extracted are detailed in an accompanying document (Mastin et al., in preparation). Some entries were also compiled by previous authors (Wilson et al., 1978; Carey and Sigurdsson, 1989; Sparks et al., 1997, Table 5.1). Our compilation includes only events of the past century or so, excludes one from previous tables (Bezmyanny, 1956) that is now known not to have produced a Plinian column (Belousov et al., 2007), and added some (e.g. Fuego, 1974; Spurr, 1992; Ruapehu, 1996; Etna, 2001) for which data have recently become available. Some large or well-documented eruptions that one might expect in this table, such as Rotomahana 1886, are omitted if information on one or more parameters is unreliable or contradictory. Each number in this table is based on an observational technique that has associated uncertainties. In particular:

*Plume height  $H$*  is, for our purposes, the elevation at which most ash spreads laterally from the plume into the ash cloud. We would generally expect this to equal the height  $H_u$  at the center of the umbrella

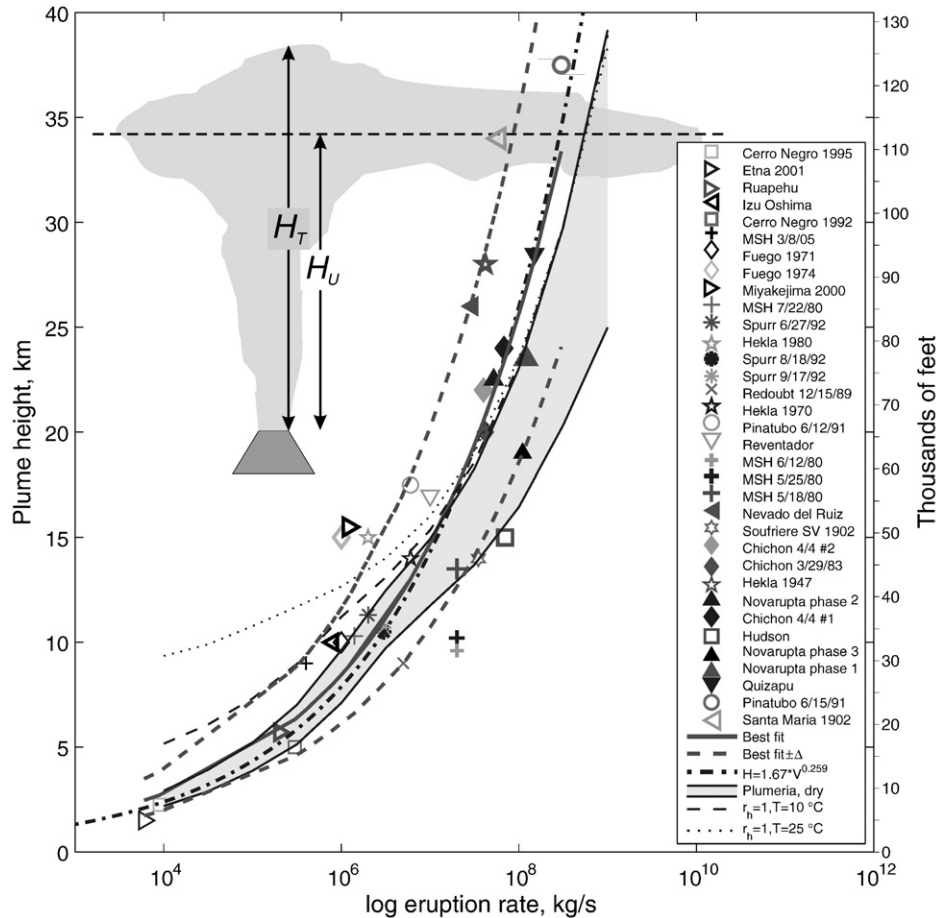


**Fig. 1.** Plume height above the vent versus mass eruption rate for eruptions listed in Table 1. Symbols for each eruption are given in the legend. The bold solid line gives the best fit to the data (Eq. (1)). The bold dashed lines enclose the error envelope ( $\pm \Delta$ ) calculated by the routine polyval in Matlab® (use of trade names does not constitute endorsement of these products). The error envelope corresponds to a 50% confidence interval, meaning that future observations have at least a 50% probability of falling within this envelope. The dot-dashed line is the empirical fit obtained by Sparks et al. (1997, Eq. 5.1). The upper light solid line is a theoretical curve of  $H_T$  calculated using the 1-D steady-state model Plumeria (Mastin, 2007) using a magma temperature of 900 °C, 3 wt% gas, and a Standard dry atmosphere (United States Committee on Extension to the Standard Atmosphere, 1976). The lower light solid curve is the elevation of neutral buoyancy, assumed to approximate  $H_U$ , calculated from the same model runs. The region between these two curves is shaded. The dashed light curve represents predictions of  $H_T$  by Plumeria using properties of a Standard atmosphere but with 100% relative humidity ( $r_h$ ) and a temperature at ground level of 10 °C. The light dotted curve is a similar prediction using a relative humidity of 100% and a temperature at ground level of 25 °C. Symbols in the legend are arranged from lowest to highest eruption rate. The Abbreviation “MSH” is Mount St. Helens, “Soufrière SV” is Soufrière de St. Vincent. The figure inset illustrates the difference between the height of the top of the plume ( $H_T$ ) and the height of the umbrella cloud ( $H_U$ ). The height  $H$  plotted includes both  $H_T$  and  $H_U$  depending on the method of estimation. Isopleth-based estimates, denoted by solid symbols, give umbrella-cloud height  $H_U$  whereas all other methods are thought to give  $H_T$ .

cloud (Fig. 1), where the bulk density of the erupting mixture equals that of the surrounding air. The umbrella cloud height is generally lower than the plume-top height  $H_T$ , although for eruption rates up to about  $10^8$  kg/s, 1-D plume models suggest that the difference is less than a few kilometers (Fig. 1). As eruption rates approach  $10^9$  kg/s,  $H_U$  and  $H_T$  may differ by more than 10 km. At Pinatubo discrepancies of up to 17 km were measured (Holasek et al., 1996).

Most plume-height observations that we have compiled are maximum plume height  $H_T$ , obtained primarily from ground-based or airborne visual observations, radar measurements, and cloud satellite temperature (Tupper and Wunderman, 2009–this volume). These methods rely on different phenomena that may occur at different heights. Visual observations track the highest visible part of the cloud, which may be ash-poor. Radar may give heights reflecting the highest particle-rich part of the plume. Temperature-based satellite plume heights use infrared cloud temperature, which is integrated through a finite distance near the cloud top, and must sometimes be corrected for thermal disequilibrium effects (Woods and Self, 1992). For eruptions where the plume was not directly observed, we use plume height estimated from isopleth patterns (Carey and Sparks, 1986). Isopleth patterns likely reflect the height of the umbrella cloud ( $H_U$ , Fig. 1) rather than the plume-top height ( $H_T$ ), and depend somewhat on the model used to derive the relationship. We indicate the plume-height estimation method in Table 1 as explained in the table caption.

Eruption duration  $D$  is considered in this paper to be the time period over which a significant amount of ash is continuously emitted into the atmosphere. The start and stop times of eruptions are estimated from visual observation, seismicity, and in some cases satellite imagery (the time when the ash cloud separates from the vent). We consider seismic durations to be more accurate than visual estimates, as ash-poor clouds may rise from a crater for hours after a drop in seismicity signals the end of significant ash emission. For some eruptions we define the end time as that when the plume height drops abruptly, even though low-level explosive activity may continue for several more hours. Similarly, for some eruptions (e.g. Cerro Negro, 1992) we include only the part of the eruption when ash emission was vigorous. We consider this justified; as a decrease in plume height by a factor of two implies nearly an order of magnitude decrease in eruption rate.

Erupted volume  $V$  (dense-rock equivalent or DRE) was obtained using whatever volume integration methods were employed in published sources without attempting to recalculate for uniformity. The tephra volume is converted to erupted mass by multiplying by an average deposit density, which was provided by the authors. A magma density of  $2,500$  kg/m<sup>3</sup>, typical of a water-saturated melt containing a few tens of percent crystals (as calculated using Conflow (Mastin, 2002)) is used to convert to DRE volume. Total deposit-volume estimates at Mount St. Helens (Durant et al., 2009) and Etna (Scollo et al., 2005), among other places, have been found to vary by more than a factor of two depending on how the thickness is integrated over the deposit area and beyond. This variation partly reflects the uncertainty in the amount of fine distal ash (Fierstein and Nathenson, 1992). When a range is given, we take a value near the middle of the range and assume an uncertainty of plus or minus several tens of percent.

### 3. Parameter relationships

With the above limitations in mind, we observe the following relationships.

#### 3.1. Plume height versus eruption rate

The relationship between plume height and eruption rate is perhaps the most extensively studied between any source parameters. Theoretical studies (Morton et al., 1956) indicate that  $H_T$  should increase with the fourth root of eruption rate, and empirical compilations (Settle, 1978; Wilson et al., 1978; Sparks et al., 1997, Chapter 5) roughly follow

this relationship. Fig. 1 plots plume height  $H_T$  or  $H_U$  (km) versus average eruption rate for the eruptions in Table 1. The best-fit line through these data (bold solid line), with mass eruption rate  $\dot{M}$  (kg/s) converted to volumetric flow rate  $\dot{V}$  (m<sup>3</sup> DRE per second), is

$$H = 2.00 \dot{V}^{0.241} \quad (1)$$

This does not differ in a statistically significant way from the best-fit equation of Sparks et al. (1997, Eq. 5.1, dot-dashed line in Fig. 1),

$$H = 1.67 \dot{V}^{0.259} \quad (2)$$

using 28 eruptions, 12 of which are included in Table 1.

More significant is the error envelope (bold dashed lines) that encloses half of the predictions (see figure caption for detail). An observed plume height of, say, 25 km correlates with a best-fit eruption rate of about  $1 \times 10^8$  kg/s; however, within this error envelope the eruption rate varies from about  $2 \times 10^7$  to  $4 \times 10^8$  kg/s—a factor of four in either direction. The scatter in the data limits the accuracy with which one might constrain eruption rate given an observed plume height.

Some scatter may result from error in plume-height measurements, but systematic errors are difficult to discern from this plot. Visually estimated plume heights such as at Hekla in 1947, which Thorarinsson (1949, p. 54) considered the top of a vapor-rich cap, are not outliers above the curve. Plume heights estimated by isopleth patterns at eight eruptions (El Chichón, Nevado del Ruiz, Quizapu, Novarupta) do not lie significantly below the curve although these data reflect umbrella cloud height  $H_U$  rather than plume-top height  $H_T$  (Fig. 1 inset).

Scatter may also result from inconsistent or inaccurate eruption-volume estimates. Perhaps the best such estimates are obtained by rapid, extensive mapping within days of an eruption as were performed following eruptions at Mount St. Helens and Fuego volcano in 1974. Less accurate measurements are likely to underestimate total volume, and indeed we see that most Mount St. Helens 1980 data points in Fig. 1 are skewed to the right of the trend, as might be expected from especially complete sampling. But the Fuego data point is skewed far to the left. The 1947 Hekla data point is similarly skewed left, although the deposit was constrained by 93 measurements collected within days of the eruption.

Scatter may also result from processes such as pyroclastic-flow activity or water vapor entrainment, but such effects are also difficult to discern. The unusually low plume height given the eruption rate of the May 18, 1980, Mount St. Helens plume was attributed by Carey et al. (1990) to the contribution of elutriated ash from pyroclastic flows that occurred at mid-day. Eruptions on May 25 and June 12, which also had associated pyroclastic flows, lie even farther below the curve. But the plume height for the June 15, 1991, Pinatubo eruption lies at or slightly above the curve, even though large concurrent pyroclastic flows almost certainly contributed to the layer C tephra volume (Dartevelle et al., 2002). For eruption rates less than about  $10^7$  kg/s in tropical conditions, plume heights are thought to be boosted by entrainment of water vapor (Woods, 1993, fine dashed and dotted curves in Fig. 1). Yet, little scatter is evident in this range of eruption rates.

Plume height, duration, and erupted volume for the 1980 Mount St. Helens eruptions, the Mount Spurr eruptions, the June 12, 1991 Pinatubo eruption, and the 2001 Etna eruption are exceptionally well constrained. Yet there is considerable scatter among just these data points, suggesting that at least some variability is real and not related to inaccuracies in measurement. Poorly-understood factors such as wind (Bursik et al., 2009), particle fallout (Woods and Bursik, 1991), vent overpressure (Ogden et al., 2008), or development of hydrometeors (Durant et al., 2009; Textor et al., 2006), along with atmospheric humidity for larger eruptions (Tupper et al., in review) may all influence this relationship. Finally, as illustrated by Barsotti and Neri (2008) at Etna, some scatter may reflect temporal variations in plume height or eruption rate that are not accurately reflected in the average values in Table 1.

### 3.2. Plume height and erupted volume

Our compilation of 34 historical eruptions shows a positive correlation between plume height  $H$ , in km, and erupted volume  $V$ , in  $\text{km}^3$  DRE (Fig. 2). The a best-fit line through these data is

$$H = 25.9 + 6.64 \log_{10}(V). \quad (3)$$

This correlation resembles that of Carey and Sigurdsson (1989) based on 40 Pleistocene and Holocene Plinian eruptions, five of which are in our list. Eruptions in their compilation are all silicic and generally larger in volume ( $0.1\text{--}150 \text{ km}^3$ ) than ours ( $0.001\text{--}8 \text{ km}^3$ ). Quantitatively, the correlation coefficient to our data (0.79) is comparable to theirs (0.77) between  $H$  and tephra-fall volume but worse than their correlation (0.87) between  $H$  and total volume of fall, surge, and pyroclastic-flow deposits.

Outliers and subpopulations in this trend may reflect different eruption processes or circumstances. The March 8, 2005 eruption at Mount St. Helens, for example, lasted much less than an hour and deposited only about  $10^{-4} \text{ km}^3$  of tephra (DRE), but sent a plume to about 9 km above the vent according to pilot reports (Houlié et al., 2005; Moran et al., in press). The plume height may have been boosted somewhat by atmospheric conditions (Mastin, 2007), while the brevity of the eruption limited deposit volume. The anomalously high plume at Nevado del Ruiz relative to its volume and eruption rate (Figs. 1 and 2) may reflect both its brief duration (Naranjo et al., 1986), and limitations of applying isopleth plume-height estimates in areas of great topographic relief around this 5.3-km-high volcano. The

higher-than-average plume at Pinatubo on June 15, 1991, in Fig. 2 seems to be without explanation. This volume represents that of tephra fall unit C<sub>1</sub> and C<sub>2</sub> of Koyaguchi and Ohno (2001a); while plume height of 35–40 km is from satellite data (Koyaguchi and Tokuno, 1993; Lynch and Stephens, 1996; Self et al., 1996). Small-volume eruptions with plume heights that lie below the best-fit curve in Fig. 2 are basaltic cinder cones that erupted for days (Cerro Negro and Etna), while the most obvious medium-sized outlier below the trend is Mount St. Helens on May 18, 1980, whose contribution from elutriated pyroclastic-flow debris may have pushed its volume well above the expected value for that plume height (Carey et al., 1990). Given this effect at Mount St. Helens, the excursion of Pinatubo above the trend, with its abundance of elutriated ash, is perplexing.

Carey and Sigurdsson (1989) interpret the correlation between plinian plume height and volume to reflect conduit widening and associated increases in mass discharge rate with time. Large magma bodies can support greater eruption rates (and higher plumes) before magma pressure is depleted. A similar mechanism may contribute to the correlation in Fig. 2.

### 3.3. Eruption duration

The observed correlations of both eruption rate and volume with plume height suggest that the duration of eruptions may not vary systematically with rate or volume. To examine this relationship we split the “silicic” eruptions in Table 1 into two by groups: (1) andesite and (2) dacite or rhyolite; and plotted a histogram of duration with magma type in Fig. 3. Among the eruptions in our list, almost half

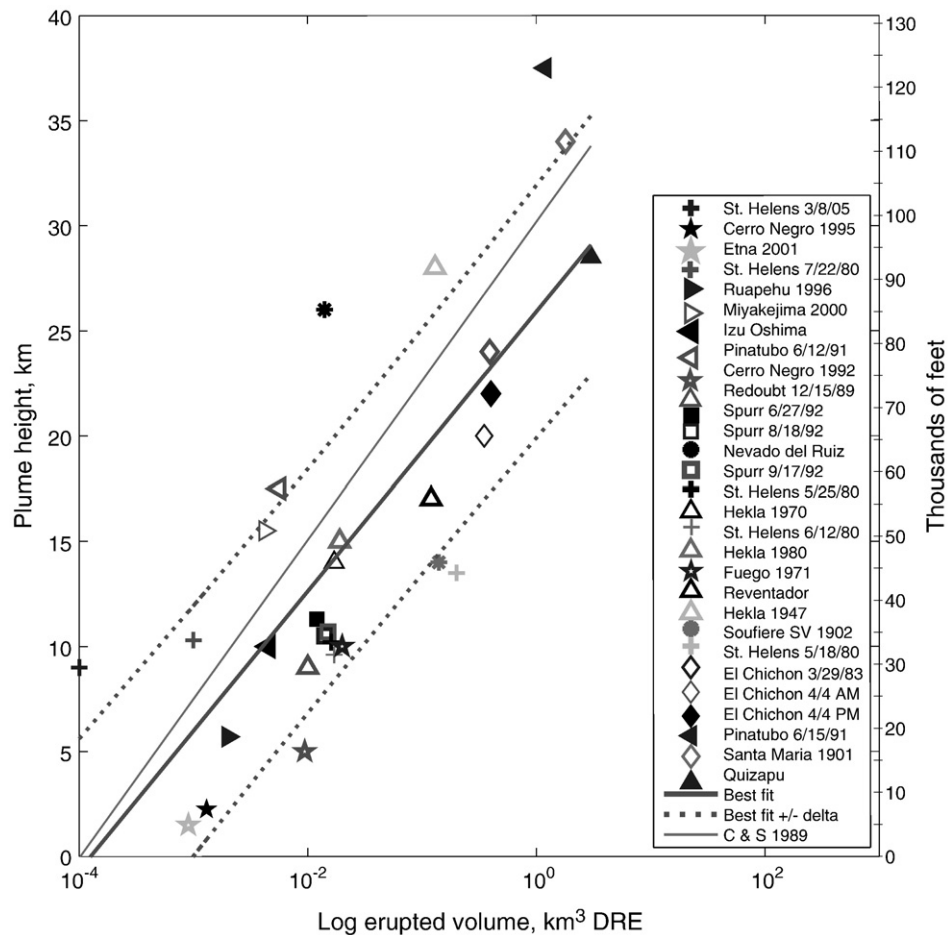
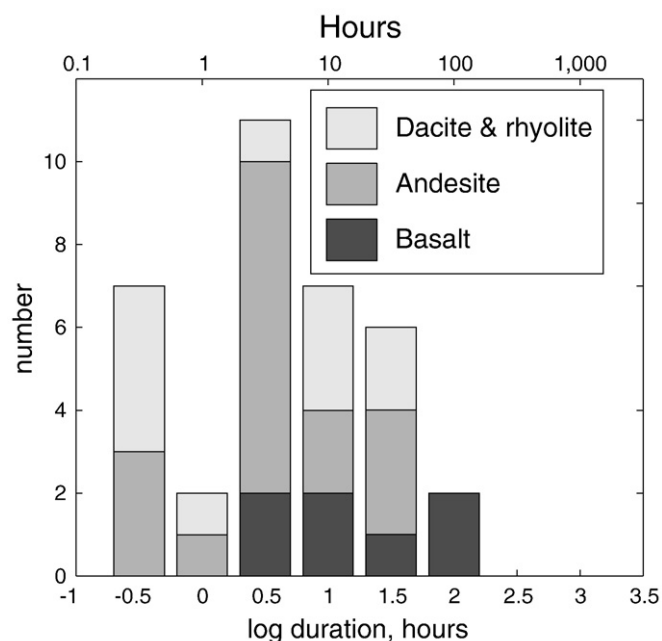


Fig. 2. Plume height versus log erupted volume (DRE) for the eruptions listed in Table 1. The bold solid line is the best-fit curve through the data, and the bold dotted lines are envelope curves that enclose 50% of the predictions as calculated by the routine polyval in Matlab®. The light solid line is the best-fit curve obtained by Carey and Sigurdsson (1989). Symbols in the legend are arranged from smallest to largest erupted volume.



**Fig. 3.** Histogram of the log of eruption duration for eruptions in Table 1. Eruptive phases for Novarupta and Hekla were combined to a single duration in this figure. Eruptions at Nevado del Ruiz and Soufrière of St. Vincent volcanoes were not included because they involved both andesite and dacite with no clear indication of which magma type was dominant (Carey and Sigurdsson, 1978; Naranjo et al., 1986).

lasted between one and ten hours. Eruptions lasting less than an hour are entirely rhyolite, dacite, or andesite, (although Strombolian bursts, if any were in this table, would be basaltic examples of this duration). Tephra eruptions lasting > 100 hours are exclusively basaltic with plume heights less than several kilometers (e.g., Cerro Negro, 1995; Etna, 2001). By contrast, the duration of large ( $VEI \geq 5$ ) silicic eruptions varies from about 3 hours for Pinatubo's most vigorous phase to a few days for eruptions at Santa Maria and Novarupta (the three phases combined).

#### 3.4. Mass fraction of fine ash

The grain-size distribution of tephra produced during an eruption is highly relevant to aviation hazards but poorly characterized. Volcanic eruptions produce fragments ranging in size from meters to fractions of a micron. Particles larger than a millimeter or so fall out at roughly their terminal velocity and are generally removed from the eruption column in the first 30 min (Rose, 1993). Finer particles fall at rates influenced by variable and poorly understood processes of particle aggregation (Carey and Sigurdsson, 1982) and hydrometeor scavenging (Slaughter and Hamil, 1970). Of greatest interest for aviation is the fraction of the erupted mass composed of fine ash, less than several tens of microns, that can stay in the ash cloud for hours or days. These are the so-called Class III particles of Koyaguchi and Ohno (2001b).

The mass fraction of fine ash can be estimated from the total grain-size distribution (TGSD) of eruptive debris. Several studies have estimated the total grain-size distribution by analysis of old tephra deposits (Suzuki et al., 1973; Walker, 1980; Sparks et al., 1981; Walker, 1981a,c; Self, 1983; Hayakawa, 1985; Woods and Bursik, 1991, Table 1). With a possible exception for phreatomagmatic tephra (discussed below), results of these studies are skewed by the fact that distal ash, which composes a significant volume of the erupted material, is eroded or too widely dispersed and unavailable for study. Accurate TGSD analyses require immediate sampling, usually within days of eruption, of a tephra that falls primarily over land. To date, only a handful of such attempts have been made.

Total grain-size distributions have generally been calculated by combining grain-size distributions from samples collected at multiple

locations throughout a deposit. TGSDs obtained by this method exclude ash that remains in the cloud for great distance and therefore tend to underestimate the mass fraction of fine ash. Moreover, TGSDs are commonly bi- or polymodal, with modes that reflect different processes of fragmentation (Carey and Sigurdsson, 1982; Durant et al., 2009). In silicic eruptions, elutriated ash clouds from pyroclastic flows are thought to produce a very fine ash mode with 5–25% of the debris < 10  $\mu\text{m}$  in diameter (Darteville et al., 2002; Durant et al., 2009). The polymodal character of TGSDs implies that the fine mass fraction (< 63  $\mu\text{m}$ ) is not accurately estimated from simple fitting statistics such as  $md_\phi$  and  $\sigma_\phi$ , which assume a Gaussian distribution with the log of diameter.

Table 2 lists the mass fraction ( $m_{63}$ ) of erupted material smaller than 63  $\mu\text{m}$  for eruptions in which TGSDs have been quantified. Values represent the mass sums from individual size classes rather than calculations based on the statistical parameters  $md_\phi$  and  $\sigma_\phi$ . The high value (0.5) for the 1980 eruption of Mount St. Helens no doubt reflects the contribution of elutriated pyroclastic-flow debris. However, values from the two 1992 Crater Peak (Mount Spurr) eruptions are only slightly lower despite the fact that pyroclastic flows were not as prominent in these eruptions.

**Table 2**

Studies where total grain-size distributions (TGSDs) and the mass fraction of tephra ( $m_{63}$ ) smaller than 63  $\mu\text{m}$  in diameter have been determined for an eruption. Entries in italics are TGSDs of phreatomagmatic eruptions, derived from analysis of old tephra deposits.

Example	$m_{63}$	Comments
Etna, 7/2001	~0.01	Measured from TGSD histogram in Scollo et al. (2007), which was derived using the Voronoi tessellation technique. Grain-size distributions of individual samples were obtained by sieve analysis, with the smallest sieves being 63 $\mu\text{m}$ .
Fuego, 1974	0.03–0.07	Taken from Table 2 in Rose et al. (2008). The range represents the variation using three methods: a modified method of Murrow et al. (1980) (0.07), the method of Murrow et al., with 10% pyroclastic-flow debris added (0.07), and the Voronoi tessellation technique (0.03).
Cerro Negro, 1968	0.12	Rose et al. (1973)
Cerro Negro, 1971	0.09	Rose et al. (1973)
Ruapehu, 1996	0.02–0.09	Measured from histograms in Fig. 3 of Bonadonna and Houghton (2005). The range reflects results of three methods: technique A, which weights the grain size distribution at each sample site by the mass per unit area at the site (0.02); technique B, similar to that of Carey and Sigurdsson (1982) at St. Helens, (0.09), and the Voronoi tessellation technique (0.03).
Taupo Hatepe A	0.34	The TGSD of this 1.8 ka phreatomagmatic eruption was estimated by analysis of the mapped deposit (Walker, 1981a, Table 1)
Taupo Hatepe B	0.36	The TGSD of this 1.8 ka phreatomagmatic eruption was estimated by analysis of the mapped deposit (Walker, 1981a, Table 1)
Towada Hachinohe HP5	0.38	The TGSD of this 13 ka phreatomagmatic eruption was estimated by analysis of the mapped deposit (Hayakawa, 1985, Table 17)
Towada Hachinohe HP1	0.42	The TGSD of this 13 ka phreatomagmatic eruption was estimated by analysis of the mapped deposit (Hayakawa, 1985, Table 17)
Towada Hachinohe HP3	0.45	The TGSD of this 13 ka phreatomagmatic eruption was estimated by analysis of the mapped deposit (Hayakawa, 1985, Table 17)
Taupo, Rotongaio	0.46	The TGSD of this 1.8 ka phreatomagmatic eruption was estimated by analysis of the mapped deposit (Walker, 1981a, Table 1)
Spurr, 8/18/92	0.3	Durant et al. (2009)
Spurr, 9/16–17/92	0.4	Durant et al. (2009)
Soufrière Hills, Montserrat	0.4–0.7	Bonadonna et al. (2002)
MSH 5/18/1980	0.5	From size fractions illustrated in Fig. 23 of Durant et al. (2009) using a mass-weighted derivation of the TGSD.
El Chichón 4/4/82	0.5	Rose and Durant (in press)

The most striking feature in this table is the variability in  $m_{63}$ , which ranges by nearly two orders of magnitude between the small mafic 2001 Etna eruption and silicic eruptions at Mount St. Helens and Soufrière Hills. The difference reflects magma type and the presence or absence of pyroclastic-flows, but could also partly result from incomplete sampling or attempts to estimate total grain-size distribution from proximal deposits. At Etna for example, distal deposits were lost in the Mediterranean.

The mass fraction of fine ash has also been estimated by indirect methods. Most notably, the crystal concentration method of Walker (1980, 1981b) suggests that medium to large eruptions can generate a mass fraction of fine ash ranging from ~0.5 to more than 0.7. In the Taupo, Hatepe, and Waimihia plinian ashes, Walker (1980, 1981a,c) estimated that 70–75% of their erupted mass consisted of fine ash, transported beyond the area of mapped deposits. Williams and Self (1983) estimated about 50% for the 1902 Santa Maria eruption. Hayakawa (1985) estimated 69% and 63% fine ash for the Chuseri and Nambu ashes, respectively. Koyaguchi and Ohno (2001a) used a modification of the crystal concentration method to estimate that 48 to 60% of Pinatubo tephra layers C<sub>1</sub> and C<sub>2</sub> was transported beyond the mapped area. The size range of these fragments is not known, hence  $m_{63}$  for these eruptions may not have differed substantially from that of medium-sized and large silicic eruptions in Table 2.

Hydromagmatic tephra deserve special mention due to their characteristic fine grain size which has been widely noted. Widespread phreatoplinian tephra show little or no size fractionation with distance from the vent, suggesting that TGSDs might be reasonably estimated from sampling and analysis of older deposits (Sparks et al., 1981; Walker, 1981a). The few such TGSDs that have been attempted, at Askja, Taupo, and Tawada volcanos (Table 2) yield  $m_{63} = \sim 0.45\text{--}0.6$ , which is similar to that of silicic non-hydromagmatic tephra. This similarity suggests that hydromagmatic eruptions need not be considered separately for our purposes.

#### 4. Eruption categories

We use this compilation to identify eleven eruption types (Table 3): small, medium, and large eruptions of mafic and silicic magma respectively; silicic co-ignimbrite (i.e. co-pyroclastic flow) plumes;

**Table 3**

Eruption types and source parameters assigned to each eruption type. The labels M1, M2, M3, S1, S2, S3, S8, S9, and U0 in the left-hand column are labels assigned to each eruption type. Type “M”, or mafic types, include basaltic and ultramafic magmas. Type “S”, or silicic types, include andesite, dacite, rhyolite, and others such as phonolite that can produce high ash columns. Submarine eruptions that occur beneath at least 50 m water depth are assigned type “U0”.

Eruption type	Example (Date as M/D/Y)	<i>H</i> (km) above vent	<i>D</i> (h)	$\dot{M}$ (kg/s)	<i>V</i> (km <sup>3</sup> )	$m_{63}$
Mafic, standard (M0)	Cerro Negro, Nicaragua, 4/13/1992	7	60	$1 \times 10^5$	0.01	0.05
Small (M1)	Etna, Italy, 7/19–24/2001	2	100	$5 \times 10^3$	0.001	0.02
Medium (M2)	Cerro Negro, Nicaragua, 4/9–13/1992	7	60	$1 \times 10^5$	0.01	0.05
Large (M3)	Fuego, Guatemala, 10/14/1974	10	5	$1 \times 10^6$	0.17	0.1
Silicic, standard (S0)	Spurr, USA, 8/18/1992	11	3	$4 \times 10^6$	0.015	0.4
Small (S1)	Ruapehu, New Zealand, 6/17/1996	5	12	$2 \times 10^5$	0.003	0.1
Medium (S2)	Spurr, USA, 8/18/1992	11	3	$4 \times 10^6$	0.015	0.4
Large (S3)	St. Helens, USA, 5/18/1980	15	8	$1 \times 10^7$	0.15	0.5
co-ignimbrite cloud (S8)	St. Helens, USA, 5/18/1980 (pre-9 AM)	25	0.5	$1 \times 10^8$	0.05	0.5
Brief (S9)	Soufrière Hills, Montserrat (composite)	10	0.01	$3 \times 10^6$	0.0003	0.6
Submarine (U0)	None	0	–	–	–	–

“brief” Vulcanian-style events possibly associated with lava-dome collapse; submarine eruptions from >50 m water depth; and “standard” values for mafic and silicic volcanoes, which are used when historical information about a volcano is unavailable. We chose not to designate categories for very large, VEI 5+ mafic and VEI 6+ silicic eruptions in Table 3, because we can think of no circumstance in which such source parameters would be assigned in the absence of significant observations. The source parameters for the standard cases are equal to those for medium-sized mafic (M2) and silicic (S2) eruptions. Symbols for each category are given in Table 3. Source parameters for each category are assigned from well-documented examples, with numbers rounded off and a few other adjustments as follows:

- For most categories, we use the plume height *H* and mass eruption rate  $\dot{M}$  of the example eruption, keeping in mind that these values would place the *H*– $\dot{M}$  relationship within the scatter shown in Fig. 1 but not necessarily on the best-fit curve. Tropopause elevation and atmospheric conditions clearly affect plume height, but for simplicity these effects are not presently considered. They will be the subject of future work.
- For brief silicic eruptions (S9), we assign plume height, erupted volume, and duration to the middle of the range described for events at Montserrat (Druitt et al., 2002), using a *H*– $\dot{M}$  relationship based on the empirical curve of Sparks et al. (1997, Eq. 5.1) and a total volume consistent with the product of eruption rate and duration.
- In cases where the mass fraction of fine debris ( $m_{63}$ ) of the example eruption is known (types M1, M3, S1–S3, and S8), we use that value. For medium-sized mafic eruptions (M2) we interpolate between M1 and M3 values. For brief silicic eruptions (S9) we use  $m_{63} = 0.6$ , which is within the range observed for Vulcanian events at Montserrat (Bonadonna et al., 2002). We also adjusted  $m_{63}$  for small mafic eruptions from the measured value of 0.01 to a more conservative 0.02 under the assumption that a more distal and extensive sampling program of the 2001 Etna tephra may have yielded a larger volume of fine ash.

#### 5. Assigning default source parameters to the world's volcanoes

In order to assign source parameters during an eruption when few observations are available, we have assigned default source parameters to each of the ~1520 Holocene volcanoes in the Smithsonian database (Siebert and Simkin, 2002–) using guidelines in Table 4. At volcanoes where the magma type of recent eruptions was known, we used it to assign “M” or “S” eruption types. When the magma type is unknown or inaccessible, we used the type of volcanic feature in the Smithsonian database as an indicator: shield volcanoes, fissure vents,

**Table 4**

Guidelines used to assign eruption types to Holocene volcanoes. The symbol *H* indicates characteristic plume height of the most recent historical eruptions. If both plume height and eruption VEI are available, the characteristic plume height is used to assign the eruption type. Otherwise the characteristic VEI is used to assign eruption type. Eruption type S8 (elutriated ash column) is assigned only during an eruption based on whether the column is collapsing, not to volcanoes based on historical activity.

Type	Magma type	Historical eruption characteristics
M0	Basalt or other mafic	insufficient historical data to characterize
M1		$H \leq 5$ km or $VEI \leq 2$
M2		$H = 5\text{--}8$ km or $VEI = 3$
M3		$H > 8$ km or $VEI \geq 4$
S0		insufficient historical data to characterize
S1	Andesite, dacite, rhyolite or other explosive composition	$H \leq 6$ km or $VEI \leq 2$
S2		$H = 6\text{--}12$ km or $VEI = 3$
S3		$H \geq 12$ km or $VEI \geq 4$
S8		active column collapse
S9		active lava dome is present
U0	All magma types	submarine vent with water depth $\geq 50$ m

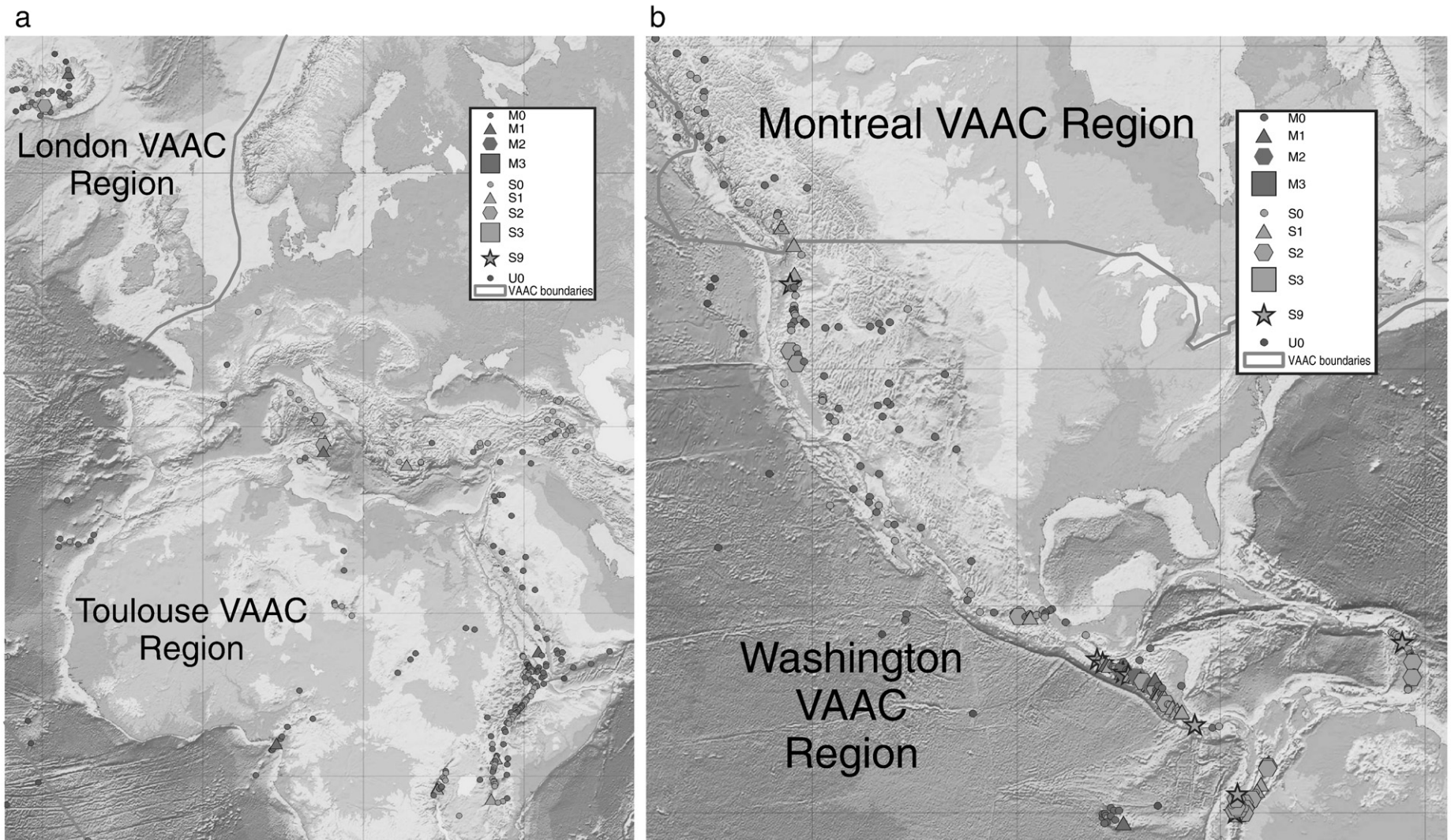


**Fig. 4.** Map of the world's Holocene volcanoes from the Smithsonian database (Siebert and Simkin, 2002–), with symbols representing the eruption type assigned to each volcano. Heavy gray lines are the boundaries of regions overseen by the various Volcanic Ash Advisory Centers (VAACs) as delineated by ICAO (International Civil Aviation Organization, 2004). Panels A through E illustrate these symbols for volcanoes in different parts of the world.



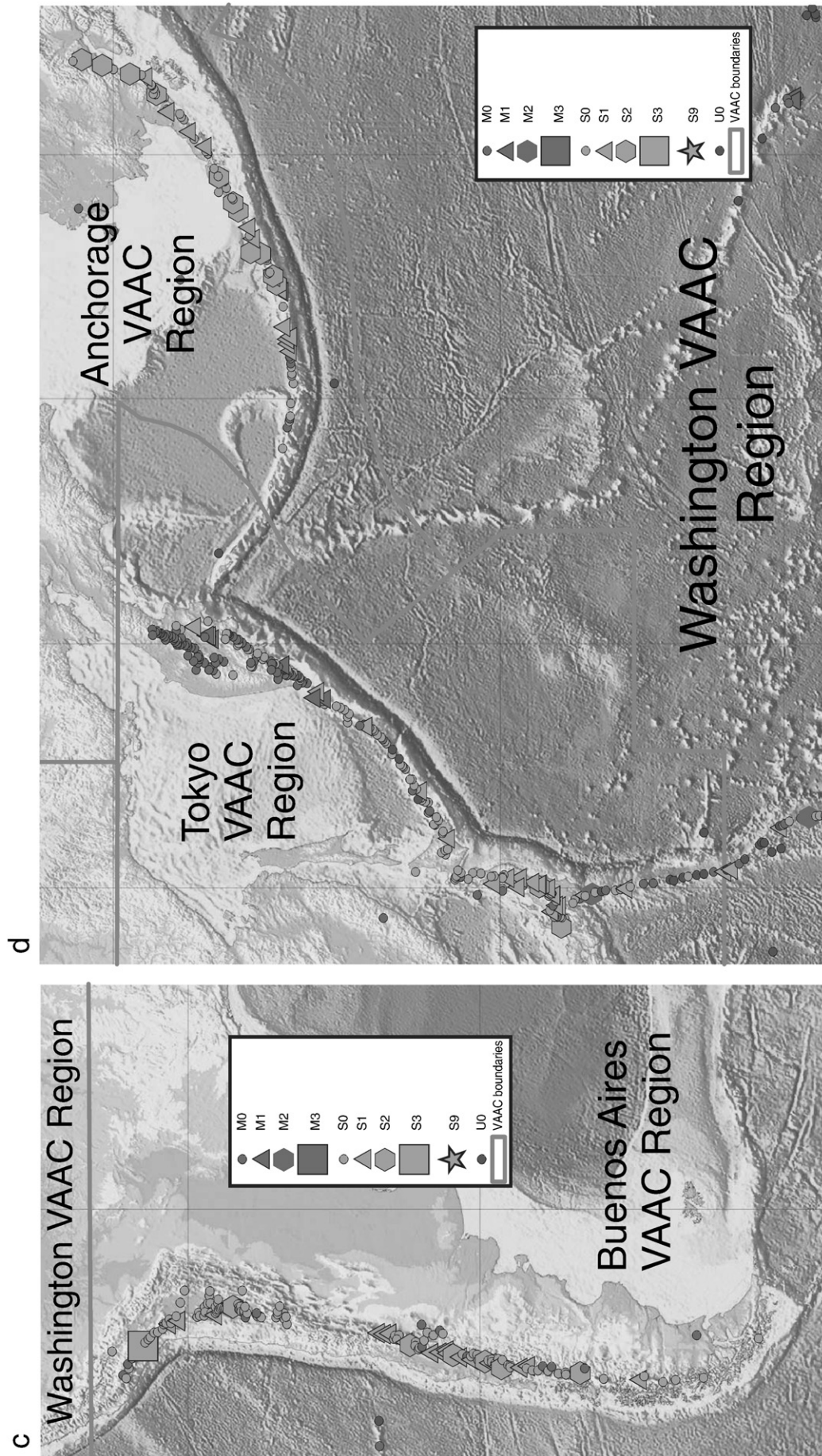


Fig. 4 (continued).

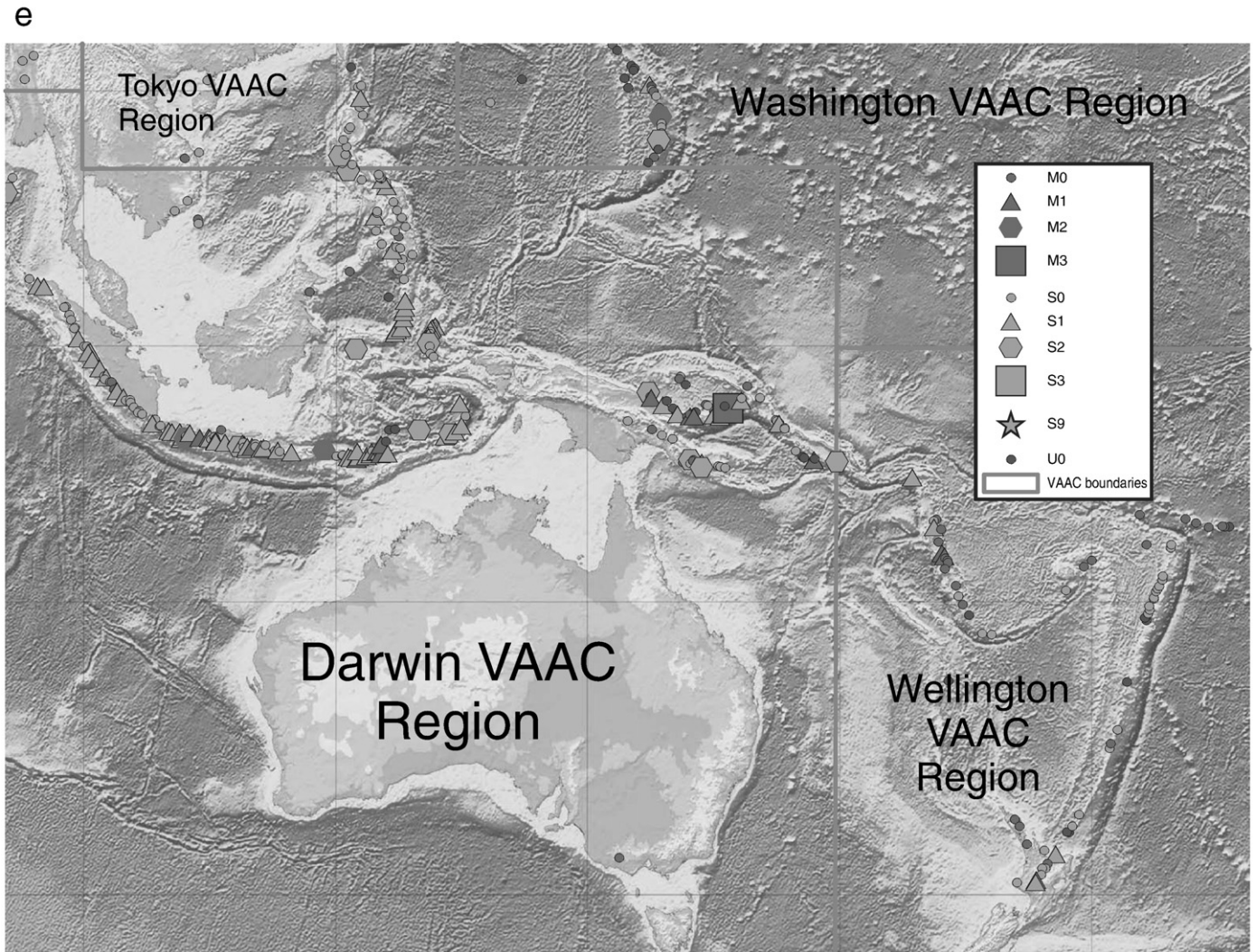


Fig. 4 (continued).

cinder cones and maars, for example were considered mafic; stratovolcanoes, lava domes, pumice cones, calderas, “complex volcanoes”, explosion craters, and bimodal volcanic fields silicic. For volcanoes with enough well-described historical eruptions to discern a trend, we assign future eruption size based on plume height of past eruptions (where available) or on the characteristic eruption size as given in the Smithsonian database using the Volcanic Explosivity Index (VEI) scale of Newhall and Self (1982). For volcanoes that had many eruptions in the past century, we gave particular weight to eruptions in the past few decades in assigning an eruption size. A spreadsheet containing these assignments will be published as an updateable document (Mastin et al., in review).

Maps of the world’s Holocene volcanoes are shown in Fig. 4, along with symbols illustrating the eruption type assigned to each one. Most volcanoes were assigned the standard categories, M0 (473 volcanoes) and S0 (663), due to lack of well-characterized historical activity (Table 5). Among those with well-described historical activity, the most common assignment was the small silicic S1 type. The decrease in the number of volcanoes assigned medium- and large eruption types reflects qualitatively the decrease in eruption frequency with increasing VEI that is well documented (Simkin and Siebert, 1994).

Although some volcanoes such as Pinatubo are characterized by large but infrequent eruptions, we assigned the large S3 type sparingly, even to those volcanoes, keeping in mind that very large (VEI $\geq$ 5) eruptions are commonly (but not always) preceded by

smaller precursory ones. Among nine VEI 5 and 6 eruptions of the twentieth century for which we have found nearby observations, six were preceded by precursory eruptions. Exceptions are Santa Maria (Sapper, 1904), El Chichón (Sigurdsson et al., 1984), and Novarupta (Hildreth, 1983). Among smaller eruptions, a disturbingly large number are not preceded by precursory eruptive activity. Simkin and Siebert (2000), for example, found that 42% of 252 historical VEI $\geq$ 3 eruptions reached their climax less than a day after the first (precursory) eruptive activity.

Table 5

Number of the world’s Holocene volcanoes assigned to each eruption category.

Category	Number
M0	473
M1	40
M2	10
M3	2
S0	663
S1	171
S2	62
S3	1
S8	0
S9	11
U0	87
total	1520

## 6. Revising source parameters during unrest and eruption

These patterns emphasize the need for volcanologists to constantly assess source parameter assignments during periods of unrest, and especially during an eruption. If new observations reveal, say, a plume height that differs from the default assignment, a simple way to adjust source parameters would be to find the eruption type in Table 3 that most closely matches the observed plume height and use the other (non-height) parameters for that type. However in general it would seem preferable for ash-cloud modeling groups to adjust parameters according to individual circumstances following consultation with volcanologists. New plume height and duration can be assigned directly based on observation. A new eruption rate might be assigned based on plume height using correlations such as Eq. (1) or 1-D plume models that consider the particular atmospheric conditions and vent elevation (Mastin, 2007). Sparse data on grain size prevent us from attempting to quantify the relationship between  $m_{63}$  and observable parameters such as plume height.

It is important to note that these assignments are rough estimates of the most likely future eruption size and type at a given volcano. No attempt is made to increase eruption size or plume height as a conservative safety factor, though we recognize that such changes affect the implied hazard. Modelers should be aware of this, as should those charged with communicating ashcloud hazards through SIGMETs or any other medium. We leave the job of adding conservatism to those charged with event response.

Future work by the Eruption Source Parameters Workgroup will involve refining eruption categories, reviewing default assignments, evaluating their utility during eruptions, and improving methods by which real-time source parameters can be assigned.

## Acknowledgments

We thank Jessica Spiegel for tirelessly helping assign source parameters to the world's volcanoes. Tina Neal, Willie Scott, Cynthia Gardner, Takehiro Koyaguchi, and Marcus Bursik added important comments in peer review, and Costanza Bonadonna provided many substantial criticisms that led to improvements. We also acknowledge the contributions of Charles Holliday, Roger Denlinger, and Cynthia Gardner, who are members of the Eruption Source Parameters Workgroup but asked not to be included as authors due to their lesser level of involvement in this part of the project.

## References

- Anderson, E.T., 1908. The Volcanoes of Guatemala. *The Geographical Journal* 31, 473–489.
- Anderson, T., Flett, J.S., 1903. Report on the eruption of the Soufriere in St. Vincent in 1902. *Philosophical Transactions of the Royal Society of London, Series A* 22, 354–553.
- Barsotti, S., Neri, A., 2008. The VOL-CALPUFF model for atmospheric ash dispersal: II. Application to the weak Mt. Etna plume of July 2001. *Journal of Geophysical Research* 113 (B03209). doi:10.1029/2006JB004624.
- Belousov, A.B., Voight, B., Belousova, M., 2007. Directed blasts and blast-generated pyroclastic density currents: a comparison of the Bezymianny 1956, Mount St Helens 1980, and Soufrière Hills, Montserrat 1997 eruptions and deposits. *Bulletin of Volcanology* 69, 701–740.
- Bonadonna, C., Houghton, B.F., 2005. Total grain-size distribution and volume of tephra-fall deposits. *Bulletin of Volcanology* 67, 441–456.
- Bonadonna, C., Mayberry, G.C., Calder, E.S., Sparks, R.S.J., Choux, C., Jackson, A.M., Lejeune, A.M., Loughlin, S.C., Norton, G.E., Rose, W.I., Ryan, G., Young, S.R., 2002. Tephra fallout in the eruption of Soufrière Hills Volcano, Montserrat. In: Druitt, T.H., Kokelaar, B.P. (Eds.), *The eruption of Soufrière Hills Volcano, Montserrat, from 1995 to 1999*. Geological Society of London, London, pp. 483–516.
- Bonis, S., Salazar, O., 1973. The 1971 and 1973 eruptions of Volcan Fuego, Guatemala, and some socio-economic considerations for the volcanologist. *Bulletin Volcanologique* 37 (3), 394–400.
- Bursik, M.I., Kobs, S., Burns, A.W., Bazanova, L., Braitseva, O., 2009. Potential effects of the jetstream on volcanic plumes: Implications for fallout and aviation safety. *Journal of Volcanology and Geothermal Research*.
- Carey, S., Sigurdsson, H., 1982. Influence of particle aggregation on deposition of distal tephra from the May 18, 1980, eruption of Mount St. Helens volcano. *Journal of Geophysical Research* 87 (B8), 7061–7072.
- Carey, S., Sigurdsson, H., 1986. The 1982 eruptions of El Chichón volcano, Mexico (2): Observations and numerical modelling of tephra-fall distribution. *Bulletin of Volcanology* 48 (2/3), 127–141.
- Carey, S., Sigurdsson, H., 1989. The intensity of plinian eruptions. *Bulletin of Volcanology* 51 (1), 28–40.
- Carey, S.N., Sigurdsson, H., 1978. Deep-sea evidence for distribution of tephra from the mixed magma eruption of the Soufriere on St. Vincent, 1902: Ash turbidites and air fall. *Geology* 6, 271–274.
- Carey, S., Sparks, R.S.J., 1986. Quantitative models of the fallout and dispersal of tephra from volcanic eruption columns. *Bulletin of Volcanology* 48, 109–125.
- Carey, S., Sigurdsson, H., Gardner, J.E., Criswell, W., 1990. Variations in column height and magma discharge during the May 18, 1980 eruption of Mount St. Helens. *Journal of Volcanology and Geothermal Research* 43, 99–112.
- D'Amours, R., Servranckx, R., Toviessi, J.-P. and Trudel, S., 1998. The operational use of the Canadian Emergency Response Model: Data assimilation, processing, storage, and dissemination. In: OECD Nuclear Energy Agency (Editor), *Nuclear Emergency Data management: Proceedings of an International Workshop*. Organisation for Economic Cooperation and Development. Nuclear Energy Agency, pp. 215–221.
- Dartevelle, S., Ernst, G.G.J., Stix, J., Bernard, A., 2002. Origin of the Mount Pinatubo climactic eruption cloud: Implications for volcanic hazards and atmospheric impacts. *Geology* 30 (7), 663–666.
- Draxler, R.R., Hess, G.D., 1998. An overview of the Hysplit-4 modeling system for trajectories, dispersion, and deposition. *Australian Meteorological Magazine* 47 (4), 295–308.
- Druitt, T.H., Young, S.R., Bapchie, B., Bonadonna, C., Calder, E.S., Clarke, A.B., Cole, P.D., Harford, C.L., Herd, R.A., Luckett, R., Ryan, G., Voight, B., 2002. Episodes of cyclic Vulcanian explosive activity with fountain collapse at Soufrière Hills Volcano, Montserrat. In: Druitt, T.H., Kokelaar, B.P. (Eds.), *The Eruption of Soufrière Hills Volcano, Montserrat, from 1995 to 1999*. The Geological Society of London, London, pp. 281–306.
- Durant, A.J., Rose, W.I., Sarna-Wojcicki, A.M., Carey, S., Volentik, A.C., 2009. Hydrometeor-enhanced tephra sedimentation: constraints from the 18 May 1980 eruption of Mount St. Helens (USA). *Journal of Geophysical Research* 114, B03204.
- Eichelberger, J.C., Keith, T.E.C., Miller, T.P., Nye, C.J., 1995. The 1992 eruptions of Crater Peak vent, Mount Spurr Volcano, Alaska: Chronology and summary. In: Keith, T.E.C. (Ed.), *The 1992 Eruptions of Crater Peak Vent, Mount Spurr Volcano, Alaska*. U.S. Geological Survey Bulletin 2139. U.S. Government Printing Office, Washington, D.C., pp. 1–18.
- Fierstein, J., Hildreth, W., 1992. The plinian eruptions of 1912 at Novarupta, Katmai National Park, Alaska. *Bulletin of Volcanology* 54, 646–684.
- Fierstein, J., Nathenson, M., 1992. Another look at the calculation of fallout tephra volumes. *Bulletin of Volcanology* 54, 156–167.
- Geshi, N., Shimano, T., Chiba, T., Nakada, S., 2002. Caldera collapse during the 2000 eruption of Miyakejima Volcano, Japan. *Bulletin of Volcanology* 64, 55–68.
- Gronvold, K., Larsen, G., Einarsson, P., Thorarinnsson, S., Saemundsson, K., 1983. The Hekla eruption 1980–1981. *Bulletin Volcanologique* 46 (4), 349–363.
- Hayakawa, Y., 1985. Pyroclastic geology of Towada volcano. *Bulletin of the Earthquake Research Institute, Tokyo* 60, 507–592.
- Hildreth, W., 1983. The compositionally zoned eruption of 1912 in the Valley of Ten Thousand Smokes, Katmai National Park, Alaska. *Journal of Volcanology and Geothermal Research* 18, 1–56.
- Hildreth, W., Drake, R.E., 1992. Volcán Quizapu, Chilean Andes. *Bulletin of Volcanology* 54, 93–125.
- Hill, B.E., Connor, C.B., Jarzempa, M.S., La Femina, P.C., Navarro, W., Strauch, W., 1998. 1995 eruptions of Cerro Negro volcano, Nicaragua, and risk assessment for future eruptions. *Geological Society of America Bulletin* 110, 1231–1241.
- Hoblitt, R.P., Wolfe, E.W., Scott, W.E., Couchman, M.R., Pallister, J.S., Javier, D., 1996. The Prelimactic eruptions of Mount Pinatubo, June 1991. In: Newhall, C.G., Punongbayan, R.S. (Eds.), *Fire and Mud: Eruptions and Lahars of Mount Pinatubo, Philippines*. University of Washington Press, Seattle, WA, pp. 457–511.
- Holasek, R.E., Self, S., Woods, A.W., 1996. Satellite observations and interpretation of the 1991 Mount Pinatubo eruption plumes. *Journal of Geophysical Research* 101 (B12), 27635–27656.
- Houlié, N., Briole, P., Nercessian, A., Murakami, M., 2005. Volcanic plume above Mount St. Helens detected with GPS. *Eos* 86 (30), 277–281.
- International Civil Aviation Organization, 2001. *Manual on Volcanic Ash, Radioactive Material and Toxic Chemical Clouds*, p. 122. ICAO Document 9691-AN/954.
- International Civil Aviation Organization, 2004. *Handbook on the International Airways Volcano Watch (IAVW): Operational Procedures and Contact List, Second Edition*, p. 113. Document 9766-AN/968.
- Jones, A., Thomson, D., Hort, M., Devenish, B., 2007. The U.K. Met office's next-generation atmospheric dispersion model, NAME III. In: Borrego, C., Norman, A.-L. (Eds.), *Air Pollution Modeling and Its Application XVII*. Springer, Berlin, pp. 580–589.
- Koyaguchi, T., 1996. Volume estimation of tephra-fall deposits from the June 15, 1991, Eruption of Mount Pinatubo by theoretical and geological methods. In: Newhall, C.G., Punongbayan, R.S. (Eds.), *Fire and Mud: Eruptions and Lahars of Mount Pinatubo, Philippines*. University of Washington Press, Seattle, pp. 583–600.
- Koyaguchi, T., Ohno, M., 2001a. Reconstruction of eruption column dynamics on the basis of grain size of tephra fall deposits: 2. Application to the Pinatubo 1991 eruption. *Journal of Geophysical Research* 106 (B4), 6513–6534.
- Koyaguchi, T., Ohno, M., 2001b. Reconstruction of eruption column dynamics on the basis of size of tephra fall deposits 1. Methods. *Journal of Geophysical Research* 106 (B4), 6499–6512.
- Koyaguchi, T., Tokuno, M., 1993. Origin of the giant eruption cloud of Pinatubo, June 15, 1991. *Journal of Volcanology and Geothermal Research* 55, 85–96.
- Lynch, J.S., Stephens, G., 1996. Mount Pinatubo: a satellite perspective of the June 1991 Eruptions. In: Newhall, C.G., Punongbayan, R.S. (Eds.), *Fire and Mud: The Eruptions*

- and Lahars of Mount Pinatubo, Philippines. University of Washington Press, Seattle, pp. 637–646.
- Mannen, K., 2006. Total grain size distribution of a mafic subplinian tephra, TB-2, from the 1986 Izu–Oshima eruption, Japan: An estimation based on a theoretical model of tephra dispersal. *Journal of Volcanology and Geothermal Research* 155, 1–17.
- Mastin, L.G., 2002. Insights into volcanic conduit flow from an open-source numerical model. *Geochemistry, Geophysics, Geosystems* 3 (7) 10.1029.
- Mastin, L.G., 2007. A user-friendly one-dimensional model for wet volcanic plumes. *Geochemistry, Geophysics, Geosystems* 8 (Q03014). doi:10.1029/2006GC001455.
- Mastin, L.G., Spiegel, J., Ewert, J. W., Guffanti, M., in review. Spreadsheet of eruption source parameters for active volcanoes of the world, U.S. Geological Survey open-file report.
- Mastin, L.G., Ewert, J.W. and Guffanti, M., in preparation. An examination of volcanic eruptions for which plume height, erupted volume, duration, and grain size are well constrained, U.S. Geological Survey Open-file report.
- McGimsey, R.G., Neal, C.A., Riley, C., 2001. Areal distribution, thickness, volume, and grain size of tephra-fall deposits from the 1992 eruptions of Crater Peak vent, Mt. Spurr volcano, Alaska, U.S. Geological Survey Open-File Report 01-0370. U.S. Government Printing Office, Washington, D.C., p. 38.
- Miller, T.P., Casadevall, T.J., 2000. Volcanic Ash Hazards to Aviation. In: Sigurdsson, H., Houghton, B.F., McNutt, S.R., Rymer, H., Stix, J. (Eds.), *Encyclopedia of Volcanoes*. Academic Press, San Diego, pp. 915–930.
- Miller, T.P., Chouet, B.A., 1994. The 1989–1990 eruptions of Redoubt Volcano: an introduction. *Journal of Volcanology and Geothermal Research* 62 (1–4), 1–10.
- Moran, S.C., McChesney, P.J. and Lockhart, A.B., in press. Chapter 6. Seismicity and Infrasonic Associated with Explosions at Mount St. Helens, 2004–2005. In: Sherrod, D.R., and Scott, W.E., *A Volcano Rekindled: The Renewed Eruption at Mount St. Helens, 2004–2006*. U.S. Geological Survey Professional Paper 1750.
- Morton, B.R., Taylor, G.L., Turner, J.S., 1956. Turbulent gravitational convection from maintained and instantaneous sources. *Proceedings of the Royal Society of London, Series A* 234, 1–23.
- Murrow, P.J., Rose, W.I., Self, S., 1980. Determination of the total grain size distribution in a vulcanian eruption column, and its implications to stratospheric aerosol perturbation. *Geophysical Research Letters* 7 (11), 893–896.
- Nakada, S., Nagai, M., Kaneko, T., Nozawa, A., Suzuki-Kamata, K., 2005. Chronology and products of the 2000 eruption of Miyakejima Volcano, Japan. *Bulletin of Volcanology* 67, 205–218.
- Naranjo, S.J.A., Moreno, R.H., Banks, N.G., 1993. La erupción del Volcán Hudson en 1991 (46° S), Región XI, Aisén Chile, Servicio Nacional de Geología y Minería–Chile, Boletín No. 44. Servicio Nacional de Geología y Minería–Chile, Santiago, p. 50.
- Naranjo, J.L., Sigurdsson, H., Carey, S.N., Fritz, W., 1986. Eruption of the Nevado del Ruiz Volcano, Colombia, on 13 November 1985: Tephra fall and lahars. *Science* 233 (4767), 961–963.
- Neal, C.A., McGimsey, R.G., Gardner, C.A., Harbin, M.L., Nye, C.J., 1995. Tephra-fall deposits from the 1992 eruptions of Crater Peak, Mount Spurr, Alaska. In: Keith, T.E.C. (Ed.), *The 1992 eruptions of Crater Peak, Mount Spurr, Alaska*, U.S.G.S. Bulletin 2139. U.S. Geological Survey, Washington, D.C., pp. 65–79.
- Newhall, C.G., Self, S., 1982. The volcanic explosivity index (VEI): an estimate of explosive magnitude for historical volcanism. *Journal of Geophysical Research* 87, 1231–1238.
- Ogden, D.E., Wohletz, K., Glatzmaier, G.A., Brodsky, E.E., 2008. Numerical simulations of volcanic jets: Importance of vent overpressure. *Journal of Geophysical Research* 113 (B02204). doi:10.1029/2007JB005133.
- Paladio-Melosantos, M.L.O., Solidum, R.U., Scott, W.E., Quiambao, R.B., Umbal, J.V., Rodolfo, K.S., Tubianosa, B.S., Delos Reyes, P.J., Alonso, R.A., Ruelo, H.B., 1996. Tephra Falls of the 1991 Eruptions of Mount Pinatubo. In: Newhall, C.G., Punongbayan, R.S. (Eds.), *Fire and Mud: Eruptions and Lahars of Mount Pinatubo*, Philippines. University of Washington Press, Seattle, pp. 513–536.
- Pallister, J.S., Hoblitt, R.P., Reyes, A.G., 1992. A basalt trigger for the 1991 eruptions of Pinatubo volcano? *Nature* 356, 426–428.
- Piedelievre, J.P., Musson-Genon, L., Bompay, F., 1990. MEDIA – An Eulerian model of atmospheric dispersion: First validation on the Chernobyl release. *Journal of Applied Meteorology* 29 (12), 1205–1220.
- Prata, A.J., Grant, I.F., 2001. Retrieval of microphysical and morphological properties of volcanic ash plumes from satellite data: application to Mt. Ruapehu, New Zealand. *Quarterly Journal of the Royal Meteorological Society* 127, 2153–2179.
- Rose, W.I., 1972. Notes on the 1902 eruption of Santa Maria volcano, Guatemala. *Bulletin of Volcanology* 36 (1), 29–45.
- Rose, W.I., 1993. Comment on ‘another look at the calculation of fallout tephra volumes’ by Judy Fierstein and Manuel Nathenson. *Bulletin of Volcanology* 55, 372–374.
- Rose, W.I. and Durant, A.J., in press. El Chichon volcano, 4 April 1982: volcanic cloud history and fine ash fallout. *Natural Hazards*. doi:10.1007/s11069-008-9283-x.
- Rose, W.I., Bonis, S., Stoiber, R.E., Keller, M., Bickford, T., 1973. Studies of volcanic ash from two recent Central American eruptions. *Bulletin Volcanologique* 37 (3), 338–364.
- Rose, W.I., Self, S., Murrow, P.J., Bonadonna, C., Durant, A.J., Ernst, G.G.J., 2008. Nature and significance of small volume fall deposits at composite volcanoes: Insights from the October 14, 1974 Fuego eruption, Guatemala. *Bulletin of Volcanology* 70, 1043–1067.
- Sapper, K., 1904. Der Ausbruch des Vulkans Santa María in Guatemala. *Centralblatt für Mineralogie, Geologie und Paläontologie* 131.
- Sarna-Wojcicki, A.M., Shipley, S., Waitt, R., Dzurisin, D., Wood, S.H., 1981. Areal distribution, thickness, mass, volume, and grain size of air-fall ash from the six major eruptions of 1980. In: Lipman, P.W., Christiansen, R.L. (Eds.), *The 1980 Eruptions of Mount St. Helens*, Washington; USGS Professional Paper 1250. U.S. Geological Survey, pp. 577–601.
- Scasso, R.A., Corbella, H., Tiberi, P., 1994. Sedimentological analysis of the tephra from the 12–15 August 1991 eruption of Hudson volcano. *Bulletin of Volcanology* 56, 121–132.
- Scollo, S., Coltelli, M., Prodi, F., Folegani, M., Natali, S., 2005. Terminal settling velocity measurements of volcanic ash during the 2002–2003 Etna eruption by an X-band microwave rain gauge disdrometer. *Geophysical Research Letters* 32 (L10302). doi:10.1029/2004GL022100.
- Scollo, S., Del Carlo, P., Coltelli, M., 2007. Tephra fallout of 2001 Etna flank eruption: Analysis of the deposit and plume dispersion. *Journal of Volcanology and Geothermal Research* 160, 147–164.
- Scott, W.E., McGimsey, R.G., 1994. Character, mass, distribution, and origin of tephra-fall deposits of the 1989–1990 eruption of redoubt volcano, south-central Alaska. *Journal of Volcanology and Geothermal Research* 62 (1–4), 251–272.
- Scott, W.E., Sherrod, D. and Gardner, C.A., in press. Chapter 1. Overview of 2004 to 2005, and continuing, eruption of Mount St. Helens, Washington. In: D. Sherrod and W.E. Scott (Editors), *A volcano rekindled: the renewed eruption at Mount St. Helens, 2004–2006*. U.S. Geological Survey Professional Paper 1750.
- Searcy, C., Dean, K., Stringer, W., 1998. PUFF: A high-resolution volcanic ash tracking model. *Journal of Volcanology and Geothermal Research* 80, 1–16.
- Self, S., 1983. Large scale phreatomagmatic silicic volcanism: a case study from New Zealand. *Journal of Volcanology and Geothermal Research* 17, 433–469.
- Self, S., Zhao, J.-X., Holasek, R.E., Torres, R.C., King, A.J., 1996. The Atmospheric Impact of the 1991 Mount Pinatubo Eruption. In: Newhall, C.G., Punongbayan, R.S. (Eds.), *Fire and Mud: The eruptions and Lahars of Mount Pinatubo*, Philippines. University of Washington Press, Seattle, pp. 1089–1116.
- Settle, M., 1978. Volcanic eruption clouds and the thermal power output of explosive eruptions. *Journal of Volcanology and Geothermal Research* 3, 309–324.
- Siebert, L., Simkin, T., 2002. *Volcanoes of the World: An Illustrated Catalog of Holocene Volcanoes and their Eruptions*. Smithsonian Institution, Global Volcanism Program Digital Information Series, GVP-3.
- Sigurdsson, H., Carey, S.N., Espindola, J.M., 1984. The 1982 eruptions of El Chichon volcano, Mexico: Stratigraphy of pyroclastic deposits. *Journal of Volcanology and Geothermal Research* 23, 11–37.
- Simkin, T., Siebert, L., 1994. *Volcanoes of the World*. Geoscience Press, Inc., Tucson, AZ. 349 pp.
- Simkin, T., Siebert, L., 2000. Earth’s volcanoes and eruptions: An overview. In: Sigurdsson, H., Houghton, B.F., McNutt, S.R., Rymer, H., Stix, J. (Eds.), *Encyclopedia of Volcanoes*. Academic Press, San Diego, pp. 249–269.
- Slaughter, M., Hamil, M., 1970. Model for deposition of volcanic ash and resulting bentonite. *Geological Society of America Bulletin* 81, 961–968.
- Smithsonian Institution, 2002. Strong, sudden 3 November eruption; 8-km-long pyroclastic flow. *Global Volcanism Program Monthly Reports*, vol. 27(11). [http://www.volcano.si.edu/world/volcano.cfm?vnum=1502-01=&volpage=var#bgvn\\_2711](http://www.volcano.si.edu/world/volcano.cfm?vnum=1502-01=&volpage=var#bgvn_2711).
- Sparks, R.S.J., Bursik, M.I., Carey, S.N., Gilbert, J.S., Glaze, L.S., Sigurdsson, H., Woods, A.W., 1997. *Volcanic Plumes*. John Wiley & Sons, Chichester. 574 pp.
- Sparks, R.S.J., Wilson, L., Sigurdsson, H., 1981. The pyroclastic deposits of the 1875 eruption of Askja, Iceland. *Philosophical Transactions of the Royal Society of London, Series A* 999, 241–273.
- Suzuki, T., Katsui, Y., Hakamura, T., 1973. Size distribution of the Tarumai Ta-b pumice fall deposit. *Bulletin of the Volcanological Society of Japan* 18, 57–64.
- Textor, C., Graf, H.F., Herzog, M., Oberhuber, J.M., Rose, W.I., Ernst, G.G.J., 2006. Volcanic particle aggregation in explosive eruption columns. Part I: Parameterization of the microphysics of hydrometeors and ash. *Journal of Volcanology and Geothermal Research* 150, 359–377.
- Thorarinsson, S., 1949. The tephra-fall from Hekla on March 29th, 1947. *The Eruption of Hekla, 1947–1948*, II, 3: The tephra-fall from Hekla on March 29, 1947. *Societas Scientiarum Islandica, Reykjavík*. 68 pp.
- Thorarinsson, S., Sigvaldason, G., 1971. The Hekla eruption of 1970. *Bulletin of Volcanology* 36 (2), 269–288.
- Tupper, A., Carn, S., Davey, J., Kamada, Y., Potts, R., Prata, F., Tokuno, M., 2004. An evaluation of volcanic cloud detection techniques during recent significant eruptions in the western ‘Ring of Fire’. *Remote Sensing of Environment* 91 (1), 27–46.
- Tupper, A., Wunderman, R. 2009. Reducing discrepancies in ground and satellite-observed eruption heights. *Journal of Volcanology and Geothermal Research* 186, 22–31 (this volume).
- Tupper, A., Textor, C., Herzog, M. and Graf, H.F., in review. Tall clouds from small eruptions: modelling the sensitivity of eruption height and fine ash fallout to tropospheric instability. *Natural Hazards*.
- United States Committee on Extension to the Standard Atmosphere, 1976. *U.S. Standard Atmosphere, 1976*. National Oceanic and Atmospheric Administration, Washington, D.C. 227 pp.
- Walker, G.P.L., 1980. The Taupo pumice: product of the most powerful known (ultraplinian) eruption? *Journal of Volcanology and Geothermal Research* 8, 69–94.
- Walker, G.P.L., 1981a. Characteristics of two phreatoplinian ashes, and their water-flushed origin. *Journal of Volcanology and Geothermal Research* 9, 395–407.
- Walker, G.P.L., 1981b. Plinian eruptions and their deposits. *Bulletin of Volcanology* 44 (3), 223–240.
- Walker, G.P.L., 1981c. The Waimihia and Hatepe plinian deposits from rhyolitic Taupo Volcanic Centre. *New Zealand Journal of Geology and Geophysics* 24, 305–324.
- Williams, S.N., Self, S., 1983. The October 1902 plinian eruption of Santa Maria volcano, Guatemala. *Journal of Volcanology and Geothermal Research* 16, 33–56.
- Wilson, L., Sparks, R.S.J., Huang, T.C., Watkins, N.D., 1978. The control of volcanic column heights by eruption energetics and dynamics. *Journal of Geophysical Research* 83 (B4), 1829–1836.
- Woods, A.W., 1993. Moist convection and the injection of volcanic ash into the atmosphere. *Journal of Geophysical Research* 98 (B10), 17627–17636.
- Woods, A., Bursik, M., 1991. Particle fallout, thermal disequilibrium and volcanic plumes. *Bulletin of Volcanology* 53, 559–570.
- Woods, A.W., Self, S., 1992. Thermal disequilibrium at the top of volcanic clouds and its effect on estimates of the column height. *Nature* 355, 628–630.